Determination of rail steel structural elements via the method of atomic force microscopy

***A. E. Balanovskiy**, Cand. Eng., Associate Prof.[1];*
***M. G. Shtaiger**, Cand. Eng., Chief operating Officer[2];*
***V. V. Kondratyev**, Cand. Eng., Senior Scientific Researcher[3];*
***A. I. Karlina**, Cand. Eng., Scientific Researcher[4], e-mail: karlinat@mail.ru*

[1]Irkutsk National Research Technical University (Irkutsk, Russia);
[2]Mechel Steel Management Company (Moscow, Russia);
[3]A. P. Vinogradov Institute of Geochemistry of the Siberian Branch of the Russian Academy of Sciences (Irkutsk, Russia);
[4]Moscow State University of Civil Engineering (Moscow, Russia)

The distance between pearlite plates is an important parameter for control of ductility and deformation strengthening of carbon steels. Most methods of optical end electronic microscopy for measuring the distances between cementite and pearlite plates in pearlite steels make definite complications when applying to high-dispersed microstructures. At present time rail steels with pearlite structure are fabricated with interlamellar distance 60-130 nm. This research used atomic force microscopy (AFM) for measuring interlamellar distances of pearlite structure in the heat-affected zone (HAZ) of rail welded joint. Qualitative evaluation of cementite and ferrite plates thickness was obtained for the first time, depending on location relating to a rail weld fusion line. The input of cementite plates in strength on the base of Hall-Petch equation was considered. Influence of the relationship between the size of pearlite colonies d_p and thickness of cementite plates t_c on metal destruction stress of a HAZ welded joint was assessed.
Keywords: structure, pearlite, ferrite, cementite, plate thickness, interlamellar distance, atomic force microscopy, rail steel, welded joint, heat affected zone.
DOI: 10.17580/cisisr.2022.01.16

Introduction

Rail steels with 100 % pearlite structure are widely used at railroad transport owing to combination of their strength and impact toughness [1-6]. High strength properties are controlled by microstructure of rail steel, especially by interlamellar distance, size of pearlite colonies and size of austenite grains [3, 4]. Pearlite is considered as important microstructure of rail steel, because it is characterized by high wear resistance, and it makes carbon the important alloying element in these steels. Pearlite is an eutectoid mixture of two phases (ferrite and cementite), which is forming during eutectoid austenite decomposition as a result of joint growth of ferrite (α) and cementite (θ) plates. It is known [1-4], that pearlite has laminated lamellar structure with relationship between thicknesses of ferrite and cementite lamellar phases as (7-8):1. However, not only pearlite amount is important, but also its morphology, i.e. shape and distance between cementite plates. The most fine is pearlite structure, the most high is its strength with the same satisfactory toughness. Thereby development of pearlite rail steels was aimed on improvement of pearlite structure via reducing interlamellar distance. Pearlite consisting of thin plates is more hard and durable than pearlite consisting of rough plates.

Plate thickness can vary approximately by 10 times (for ferrite – from 0.1 to 1.0 μm) for different heat treatment processes; the thinner are plates, the more they are distorted. Increase of ferrite microstructure dispersity enlarges amount of ferrite and cementite plates, which participate in plastic deformation and provide deformation uniformity, increasing thereby ductility [1, 3]. In order to obtain optimal relationship between strength and ductility levels, it is important to know influence of pearlite dispersity degree of the features of deformation behaviour of its structural components and, respectively, of pearlite steel. Rail pearlite steels are used for obtaining continuous welded rail at the railroad transport. Continuous welded pearlite rails (CWR) are widely used at railroads, where flash butt welding is the main method of connection [7-13]. Welded joint is the most critical area, because its destruction was observed in many researches [8-10]. There are a lot of works dedicated to welding technological features [8-13], but small amount of researches is devoted to examination of pearlite structure in the heat-affected zone (HAZ) of rail welded joint. The results of electron microscopy of pearlite structure in HAZ are presented in the works [7, 9] and good prospects of this research method are displayed. Classic metallographic methods, which are widely used for measuring the distance between pearlite plates, were examined in the works [1, 2], where it was shown that investigation of thin foil samples or shadowed carbon copies via scanning electron microscopy (SEM) is the most universal method.

Interlamellar distance is the most frequent parameter for characterization pf pearlite structures; it is measured using electron micro-pictures or fluorescent microscope screen.

The method for measuring the interlamellar distance is concluded in searching pearlite colonies with minimal distance between them and in calculating the number of plates which are crossed under straight angle by the diameter line of a drawn circle with known dimension on fluorescent screen of the microscope [1-6, 14-18]. Another method includes similar measurements made on SEM micro-pictures with preset magnification. Both methods require qualified selection of observation places, especially for deformed pearlite structures. One more difficulty is connected with these measuring methods: preparation of samples for observation using SEM technique is not simple task and needs large experience in selection of preparation methods which are suitable for the concrete set of electron microscope operating conditions. Total procedure takes much time and is low acceptable for industrial conditions.

The methods which are usually used in conventional optical microscopy are strongly restricted by resolution ability of optical microscopes and cannot be used for measuring the interlamellar distance less than 0.2 μm in modern rail steels [7-12]. At the same time, more accessible methods for examination of pearlite structure can be suggested, e.g. atomic force microscopy (AFM). High resolution, simple preparation of the samples and more simple operating procedure of atomic force microscopy together with its low cost make it rather attractive for replacement of scanning electron microscopy in such researches. Atomic force microscopy is used for analysis of quantitative and qualitative data which are based on different properties, such as morphology, size surface roughness and texture. It should be mentioned that AFM image allows fixing of very small sizes, both for cementite grains and plates. Earlier AFM was not used applying to examination of rail welded joint metal.

The aim of this work was determination of the distance between ferrite and cementite plates in the structure of eutectoid rail steel, in the area of welded joint, using atomic force microscopy.

Experimental technique

The samples of welded joint from K76F rail steel were examined in this work according to the GOST R 51685-13. Welding of DT350 rails for continuous welded rail track was conducted at rail welding plants by resistance butt machines of MSR-6301 and K-1000 types. The rail samples were prepared for examination at the rail welding plant No. 13 of RSP-M JSC (Chelyabinsk). The 5-coordinate milling processing center DMG HSC75V Linear was used for samples preparation. Cutting, scarfing and polishing of samples was conducted using the labour equipment of Struers company. Pickling of polished sections for structure reveal was executed in 3% solution of nitric acid. Optical microscopes Micromed MET-2 and Axio Scop M2m (Carl Zeiss) with magnification by 50-1,000 times were used for microstructure study. Electron microscopy was provided using JIB-4501 JEOL electron microscope. Surface topography was controlled via scanning probe microscope Solver P47- PRO of NT-MDT company in "semi-contact" scanning mode.

Obtained results

Measuring the distance between pearlite plates were conducted in different positions from the smelting line: the area of grains growth (1-2 mm from the central seam line); the area of grains comminution (8 mm from the smelting line); the area of partial transformation (12-14 mm from the smelting line) and the main metal. AFM scan with topography of pearlite structure near the smelting line is presented on the **Fig. 1.** It is shown that interlamellar distance differs seriously in several colonies which are seen on this scan. Cementite plates in one colony (see the lower part of the scan) are characterized by straightness and minimal interlamellar distance, while in the central area the plates are deformed with larger values of interlamellar distance. Ferrite and cementite small plates can be seen between cementite plates, which are emphasized in contrast mode on the scan image. Investigations in different HAZ areas of a welded joint were passed afterwards; they provided more detailed information about pearlite properties (interlamellar distance, thickness of cementite and ferrite plates). Interlamellar distance varies within the range 0.13-0.18 μm, most of colonies have interlamellar distance approximately 0.24-0.30 μm.

The studies displayed that location of structural components within the whole heat-affected zone is not homogeneous, there are morphological features. Pearlite dispersity does not meet evidently the requirements for rail steels (GOST 51685-2013), it corresponds to 3-5 points within the HAZ area according to the table 4 of the GOST 8233-56. At the same time, pearlite with 1.2 points structure according to the GOST 8233-56 can be seen. Pearlite microstructure in longitudinal and transversal directions also varies.

AFM scans with distinct images of cementite plates are shown on the **Fig. 2**, *a*. Two images in 2D plane are given on the **Fig. 2**, *b* and *c*, while the lower scan presents 3D image. Profiles of pearlite grains for each alloy are built via AFM

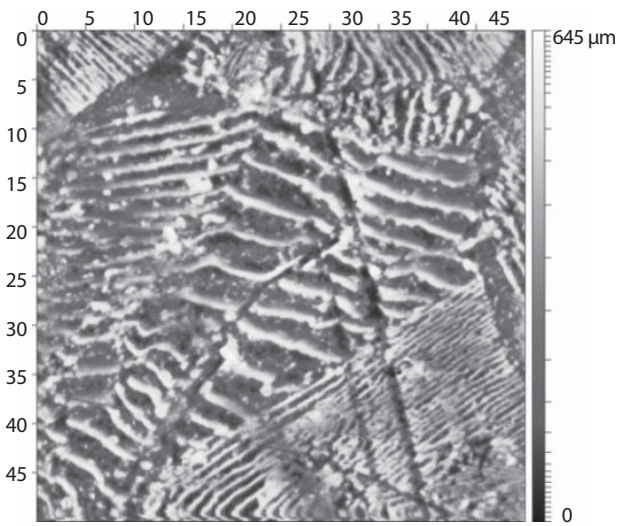

Fig. 1. AFM scan of metal surface in the area of HAZ smelting line

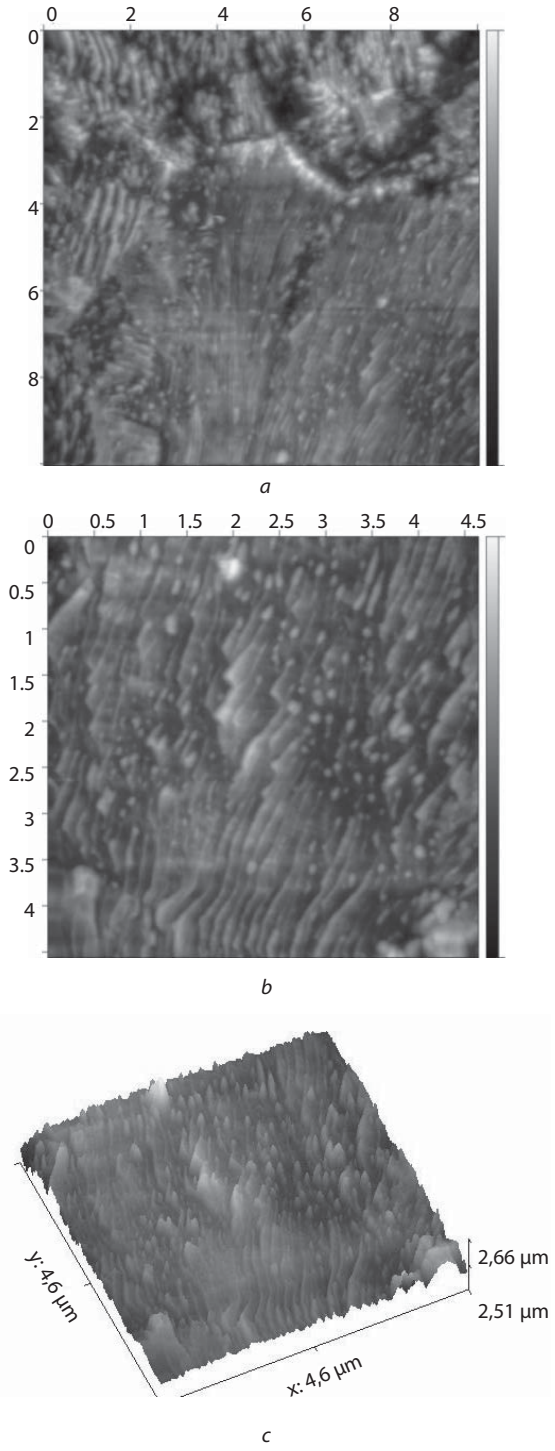

Fig. 2. Scans of AFM pearlite colonies in 2D and 3D images

images (**Fig. 3**) and dissolution depth of ferrite matrix of pearlite is calculated; it increases with enlargement of interlamellar distance as summarized thickness of ferrite and cementite plates. The testing line which is perpendicular to alternating plates (see Fig. 3, *b*) was created after selection of images from such colony. The system also suggests possibility of measuring the distances between the markers applied on such profile. Correct location of these markers allows to measure the distances between the centers of neighbor cementite or ferrite plates. Three testing lines were done for each selected pearlite colony and the average value of interlamellar distance in this colony was determined. Then the image analyzing system provided topographic control of microstructure along the line, as it is shown on the Fig. 2, *c* and d. Heterogeneity of interlamellar distance is seen well on the Fig. 3, *c*.

Cementite phase (plate) is presented by the peaks (Fig. 3, *c*). Required location of these markers allows measuring the distance between the centers of neighbor cementite plates (Fig. 3, *c* and *d*). Topographic graph of height profile, which is provided by the image analyzing system, displays distinctly the "hills" of cementite phase, which are seen on the corresponding image. The height profile was used then for calculation of interlamellar distance in rail steels, for different HAZ areas of welded joint. Visualization of pearlite structure even without quantitative measurement displays heterogeneity of the main parameters of pearlite structure morphological features via interlamellar distance as well as thickness of ferrite and cementite plates.

Discussion of the results

It was noted in the work [18] that fixing morphological cementite diversity during plastic deformation of completely pearlite steel is caused by different connection variants for plates and, probably, by lowered carbon content in local austenite areas, where the colonies having boundaries with free ferrite appeared from austenite. Topographic images of pearlite structure, obtained via AFM in different seam sections, display that the areas of grains growth in the HAZ are characterized by rather smaller interlamellar distance in comparison with the area of grains comminution; the average values make 0.12-0.014 µm and 0.17-02 µm respectively. The results of thickness measurements of cementite and ferrite plates in different sections of welded joint which were heated up to preset temperatures are presented on the **Fig. 4**. It can be seen that decrease of cementite and ferrite plates thickness occurs within the area of thermomechanical affect, during the process of flash butt welding under temperature conditions 1300 °C and above it.

It was found out that thickness of cementite plates increases with rise of austenitization temperature. Higher deformation rates in the area adjacent to the smelting line finalizes in decrease of interlamellar gap and cementite thickness. Total volumetric ferrite percent lowers, while volumetric pearlite percent with degenerated morphology elevates as soon as deformation speed rises. New modification of pearlite with partial cementite spheroidizing appears in the area of partial HAZ austenitization of welded joint [10-17].

In the work [19] the authors connected high strength in pearlite steels with close distance between cementite plates (or fragments), based on the proposal that cementite is a barrier for slipping of dislocations, similar to grains boundaries in polycrystalline iron. Cementite plates play the role in slipping restriction for dislocations, the same as influence of grain boundaries in polycrystalline takes place [1, 2, 19]. The effect of boundary strengthening, which is connected with grain size diminishing, is mainly explained by two fac-

tors: essential decrease of volume, which is available for forming of population of dislocations on the boundaries, and substantial increase of slipping resistance for deformations. Varying the interplane distance occurs mainly due to plastic deformation and thickness decrease of ferrite plate. Thickness decrease of cementite plates is typical for cementite from fine-plated pearlite; it can be subjected ti significant plastic deformation [1, 2, 19], what displays on quick transfer of plastic deformation during slipping. In this case bending of cementite plates takes place and morphology of cementite phase varies, i.e. plate form of carbide phase transforms step-by-step in bending one, owing to shift of local microvolumes in the strips of localized plastic deformation. The typical cementite structure in the area of smelting line, where high-temperature plastic deformation occurred on the final welding stage, is shown on the **Fig. 5**. Number of sections with pearlite structure having strong bended cementite plates increases together with elevation of deformation degree close to the smelting line of welded joint.

The input of cementite plates in forming of strength properties is evaluated on the base of the Hall-Petch equation, which connects the yield strength ($\sigma_т$) with the distance between barriers; it can be an obstacle for slipping of dislocations. Previous studies showed that this relationship is correct for the case of polycrystalline metals, where barrier distance is equal to grain size [1-3, 14, 18-20]. As soon as motion of dislocations occurs mainly in ferrite, the distance between the barriers is suggested larger by two times than the width of ferrite plates [1, 2]. Applying this equation to pearlite, we accept the distance between the barriers equal to average length of free path of dislocations; this length is assessed two times larger than the width of ferrite plates (*d*) [15, 16]:

$$\sigma_т = \sigma_0 + k \cdot 2\lambda^{-1/2}$$

Modified Hall-Petch relationship for cold-deformed pearlite steel can provide satisfactory description of relation between strength and microstructure. That's why the input of pearlite structural components (λ, D_F and D_C) in the level of yield strength is just true for study of the features of structure forming based on the width of ferrite plate. As soon as pearlite yield strength corresponds to stress, which is required for motion of dislocations in ferrite between to non-permeable cementite plates, it increases with reducing of interlamellar distance that leads to strengthening. This explanation is based on suggestion that the sources of dislocations are activated on the boundaries of cementite – ferrite phase separation and their motion is controlled by the length of free path <L>, which is completely equal to interlamellar distance λ. As a result, when the distance between the plates is large, dislocations can more easily transfer in the ferrite area, what leads to lowering of the yield strength and tensile strength. In general case, destruction of steel with pearlite structure can start both from a micro-crack, appearing during cutting of cementite plate, and a crack, originating on the boundaries of the colonies. The model [19] describing destruction ofplate pearlite via the micro-shearing distortion mechanism shows [19, 20] that the value of destruction stress

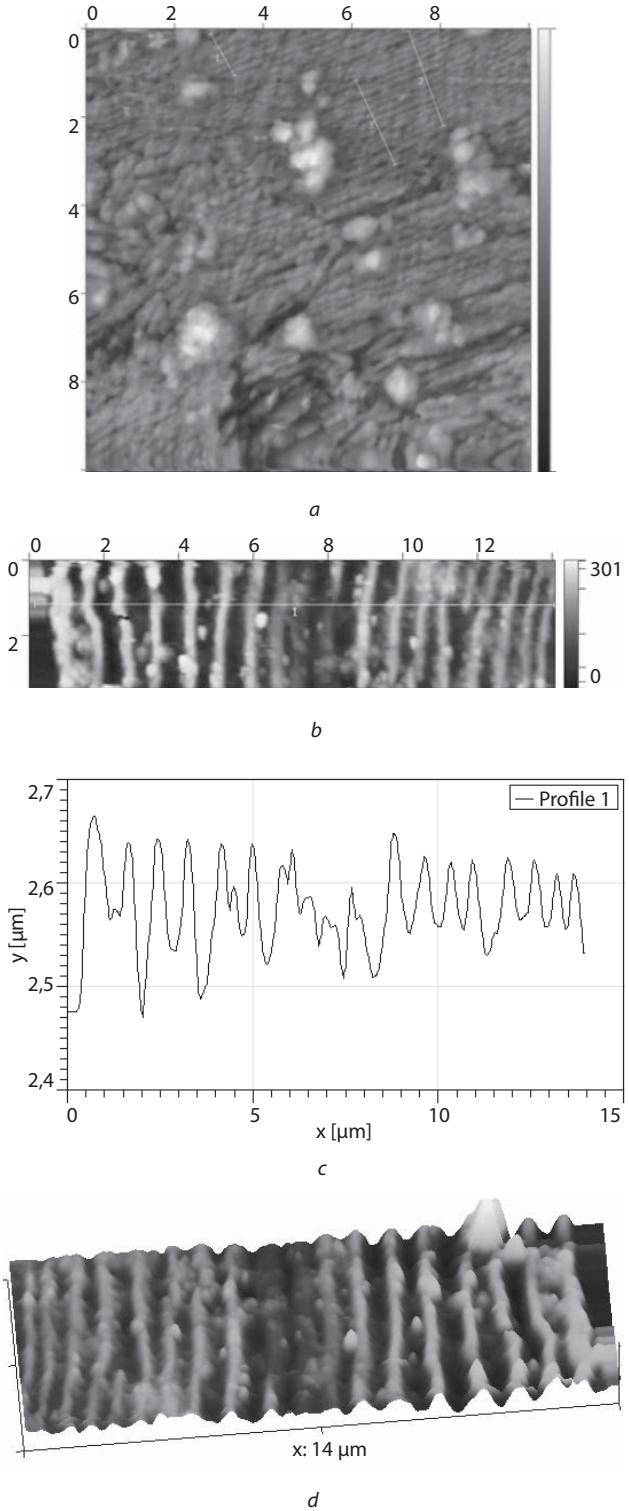

Fig. 3. Topographic profile of cementite and ferrite plates in the structure of ferrite colony

for heterogeneous crack origination (variant 1) is determined by thickness of cementite plate: $\sigma = 0.78\, t^{-1/2}$. Stress of brittle destruction on the boundary of pearlite colony depends on its size: $\sigma = 0.18\Pi^{-1/2}$. The authors of [20] think that the value of destruction stress is stipulated by selection between two structural factors as a result of competition of two mecha-

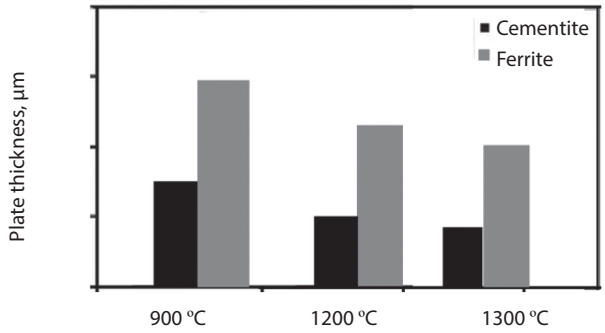

Fig. 4. Results of measuring thicknesses of ferrite (right columns) and cementite (left columns) plates in different HAZ areas using AFM

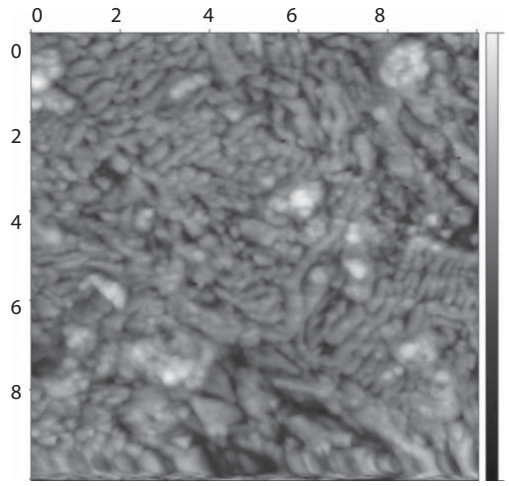

Fig. 5. AFM scan of degenerated and bended cementite in the HAZ area of welded joint

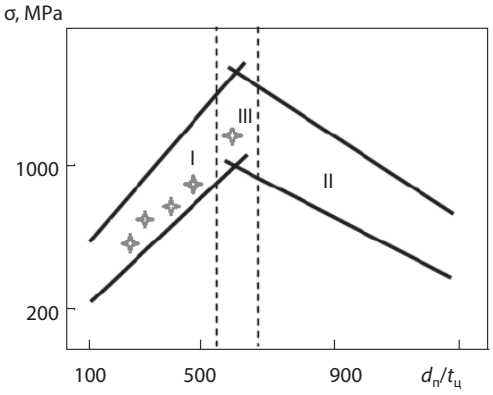

Fig. 6. Calculated relationship of influence of the size of pearlite colonies and thickness of cementite plates on destruction stress

nisms: the question is, which of these two factors (a colony or a cementite plate) will provide larger crack.

Critical relationship between the size of pearlite colonies and thickness of cementite plate, providing equal possibility of destruction from both sources, is determined be the expression $d_p/t_c = 550$. We executed calculations according to a.m. formulas and stand the results in the operating timetable [20]. Influence of the relationships between the size of pearlite colonies d_p and thickness of cementite plates tc on destruction stress of HAZ metal of welded joint is displayed on the **Fig. 6** (cross signs).

According to description of the model presented in the work [20], the area *I* on the Fig. 6 corresponds to structures, where cementite plates are the sources of micro-cracks. Pearlite colonies have determining effect on destruction processes in the area *II*, and the area *III* reflects changes of homogenous and heterogeneous sources of micro-shearing distortion [1, 2].

Obtained experimental results on measuring the thickness of cementite plates using AFM allow considering about most possible places of critical cracks origination in the areas of HAZ metal of a rail welded joint. However, additional investigations are required in this direction, using additional methods, for more detailed prediction. At the same time, the presented results can be useful for plant laboratories, for practical use of the method of atomic force microscopy in rail production, in particular for structure quality evaluation at the technological stages after rolling, heat treatment, welding etc.

Conclusions

1. The images of pearlite microstructure of rail steel samples in the heat-affected zone of a welded joint were obtained and processed using atomic force microscope. It is underlined on the base of conducted studies that the applied method is considered as a reliable tool for quantitative evaluation of interlamellar distance in pearlite structure in the heat-affected zone of rail welded joint.

2. It was established the method of atomic force microscopy allows providing of topographic profile of cementite and ferrite plates via the built-in system for analysis of obtained images. This profile is more correct and objective in quantitative dimension in comparison with conventional measuring methods of optical and electronic microscopy.

3. It is shown that thickness of cementite plates in the heat-affected zone depends on metal austenitization temperature in the area of welded joint during welding and cooling. At higher deformation rates, during upsetting in the process of welding, decrease on cementite interlamellar gap and thickness occurs in the area adjacent to the smelting line. Total ferrite volumetric percent reduces, while pearlite volumetric percent with degenerated or distorted morphology increases with enlargement of deformation rate.

REFERENCES

1. Tushinskiy L. I., Bataev A. A., Tikhomirova L. B. Pearlite structure and construction strength of steel. Novosibirsk : Nauka. 1993. 280 p.
2. Schastlivtsev V. M., Mirzaev D. A., Yakovleva I. L. et al. Pearlite in carbon steels. Ekaterinburg : UrO RAN. 2006. 132 p.

3. Yuryev A. A., Gromov V. E., Ivanov Yu. F., Rubannikova Yu. A. Structure and properties of long-size rails with differential quenching after extremely durable operation. Novokuznetsk : Poligrafist. 2020. 253 p.
4. Gromov V. E., Yuriev A. B., Morozov K. V., Ivanov Yu. F. Microstructure of quenched rails. Cambridge : CISP Ltd. 2016. 153 p.
5. Sahay S. S., Mohapatra G., Totten G. E. Overview of pearlitic rail steel: Accelerated cooling, quenching, microstructure, and mechanical properties. *Journal of ASTM*. 2009. No. 6, pp. 1–26.
6. Modi O. P., Deshmukh N., Mondal D. P., Jha A. K., Yegneswaran A. H., Khaira H. K. Effect of interlamellar spacing on the mechanical properties of 0.65 % C steel. *Materials Characterization*. 2001. Vol. 46, pp. 347–352.
7. Porcaro R. R., Faria G. L., Godefroid L. B., Apolonio G. R., Cândido L. C., Pinto E. S. Microstructure and mechanical properties of a flash butt welded pearlitic rail. *Journal of Materials Processing Technology*. 2019. Vol. 270. pp. 20–27.
8. Shtayger M. G., Balanovsky A. E., Kondratev V. V., Karlina A. I., Govorkov A. S. Application of scanning electronic microscopy for metallography of welded joints of rails. *Advances in Engineering Research Proceedings of the International Conference "Aviamechanical engineering and transport" (AVENT 2018)*. 2018. pp. 360-364.
9. Mansouri H., Monshi A. Microstructure and residual stress variations in weld zone of flash-butt welded railroads. *Science and Technology of Welding and Joining*. 2004. Vol. 9. No. 3. pp. 237–245.
10. Kuchuk-Yatsenko S. I., Didkovskiy A. V., Shvets V. I., Rudenko P. M., Antipin E. V. Contact butt welding of high-strength rails from modern production facilities. *Avtomaticheskaya svarka*. 2016. Vol. 753. No. 5-6. pp. 7-16.
11. Balanovsky A. E., Shtaiger M. G., Kondratev V. V., Karlina A. I., Govorkov A. S. Comparative analysis of structural state of welded joints rails using method of Barkhausen effect and ultrasound. *Journal of physics: conference series*. 2018. pp. 012006.
12. Nishikawa L. P., Goldenstein H. Divorced Eutectoid on Heat-Affected Zone of Welded Pearlitic Rails. *JOM*. 2019. Vol. 71. pp. 815–823. DOI: 10.1007/s11837-018-3213-5.
13. Weingrill L., Krutzler J., Enzinger N. Temperature field evolution during flash-butt welding of railway rails. *Materials Science Forum*. 2016. Vol. 879. pp. 2088–2093. DOI: 10.4028/www.scientific.net/MSF.879.2088.
14. Marder A. R., Bramfitt B. L. The effect of morphology on the strength of pearlite. *MTA*. 1976. No. 7. pp. 365–372. DOI: 10.1007/BF02642832.
15. Gridnev V. I., Gavrilyuk V. G., Meshkov Yu. Ya. Strength and ductility of cold-deformed steel. Kiev : Naukova dumka. 1974. 237 p.
16. Izotov V. I., Pozdnyakov V. A., Lukyanenko E. V., Usanova O. Y., Filippov G. A. Influence of the pearlite fineness on the mechanical properties, deformation behavior, and fracture characteristics of carbon steel. *Physics of Metalls and Metallography*. 2007. Vol. 103. No. 5. pp. 519–529.
17. Embury D., Fisher R. M. The structure and properties of drawn pearlite. *Acta Metallurgica*. 1966. Vol. 14. Iss. 2. pp. 147–159.
18. Meshkov Yu. A., Pakharenko G. A. Metal structure and brittleness of steel products. Kiev : Naukova dumka. 1985. 265 p.
19. Gridnev V. N., Gavrilyuk V. G. Cementite decomposition during steel plastic deformation (review). *Metallofizika*. 1982. Vol. 4. No. 3. pp. 74-86.
20. Tereshchenko N. A. et al. Development of rotation model of plastic deformation during drawing of pearlite steels with different alloying systems, *Fizika metallov i metallovedenie*. 2015. Vol. 116. No. 3. pp. 289–299.